Journal of Electrical and Computer Engineering Innovations
(JECEI)
Journal homepage: http://www.jecei.sru.ac.ir

Research paper

Development of Wind Turbine Fault Analysis Setup based on DFIG Hardware in the Loop Simulator

M. Kamarzarrin[1], M. H. Refan[1,2,], P. Amiri[1], A. Dameshghi[1,2]*

[1]*Faculty of Electrical Engineering, Shahid Rajaee Teacher Training University, Tehran, Iran.*

[2]*MAPNA Electric & Control, Engineering & Manufacturing Co. (MECO), Alborz, Iran.*

Article Info

Article History:
Received 16 July 2022
Reviewed 15 October 2022
Revised 29 October 2022
Accepted 07 November 2022

Keywords:
Wind turbine
HIL
DFIG
Rotor electrical asymmetry
Inter-turn short circuit
IGBT open-circuit

*Corresponding Author's Email Address: *refan@sru.ac.ir*

Abstract

Background and Objectives: Renewable energy, like wind turbines, is growing rapidly in the world today due to environmental pollution, so their maintenance plans are very important. Fault diagnosis and fault-tolerant approaches are typical methods to reduce the cost of energy production and downtime of Wind Turbines (WTs).

Methods: In this paper, a new Hardware In the Loop (HIL) simulator based on Double Feed Induction Generator (DFIG) for fault diagnosis and fault-tolerant control is proposed. The system developed as a laboratory bed uses a generator with a power of about 90 kW, which is connected from two sides to a back-to-back power converter with a power of one-third of the generator power. The generator is connected to a motor as a propulsion and wind energy replacement with a power of about 110 kW, and this connection is established through a gearbox with a gear ratio of more than three.

Results: The effectiveness of the proposed simulator is evaluated based on different fault representations back-to-back converter and generator.

Conclusion: The experiment shows that the Condition Based Maintenance (CBM) is improved by the proposed simulator and the fault is modeled before serious damage occurs. This setup is effective for the development of wind turbine fault analysis software. As the testing on real WTs is very expensive, to improve and develop the research fields of condition monitoring and WT control, this low-cost setup is effective.

Introduction

Among renewable energies, wind energy is paramount and this energy now plays a significant role in the world economic equations. Regarding the high number of Wind Turbine (WT) components, it has many faults [1], [2]. Considering the development of WT, due to the rotating equipment, fault detection, and prediction are very important in these systems. Due to the installation locations of WTs, their repairs are challenging and this equipment has a variety of electrical and mechanical failures. due to their installation place [3]-[5]. Condition-Based Maintenance (CBM) is including the CM module, Fault Detection (FD) module, fault isolation module, fault prognosis module, and fault-tolerant module (Based on Fig. 1) [3]. A study based on fault analysis is performed on different turbines. Based on this study the turbine power increase is directly related to the increase in the fault rate over a year [6]. Fig. 2 shows the failure rates of different WT components in separate studies [7]. From this figure, it is clear that the electrical failure rate is high, and of course, the highest damage and shutdown is in the gearbox, generator, blade, and propulsion. Electrical components have the highest fault rates and the lowest

shutdown rates. That is, considering that the failure rate is high in the electrical sector, but the damage and shutdown are greater in other areas [8]. Mechanical subsystems including gearboxes, blades, and generator components have low fault rates but high shutdown rates [9].

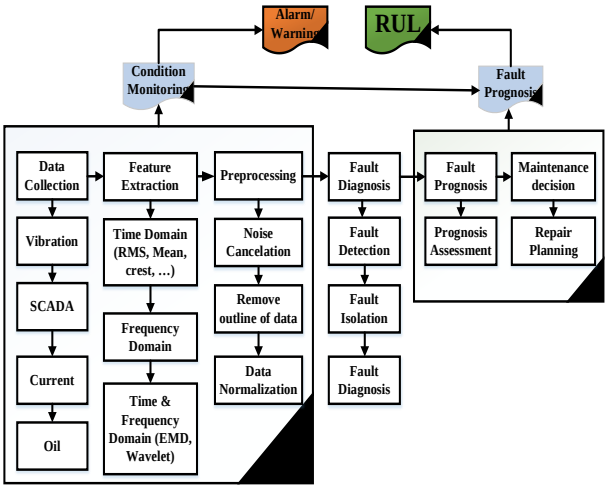

Fig. 1: Different modules in CBM.

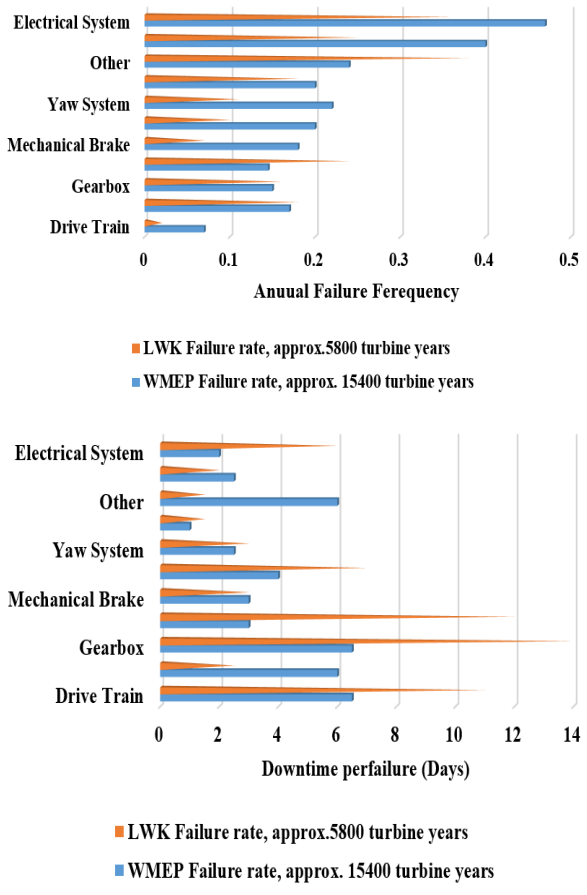

Fig. 2: Relationship between fault frequency and shutdown results from two studies on European WTs during 13 years [13].

This does not mean poor design of these parts, but due to the functional complexity and hardware of these parts [10]. The two main components, the generator, and the gearbox are very important in the reliability of the entire WT system [11]. 75% of faults cause only 5% of shutdowns, while only 25% of faults cause 95% of shutdowns [12]-[14].It is known that in small and medium-sized turbines, the faults related to the rotor and the slip ring are significant compared to the total faults of the generator, while the bearing fault is more limited [13], [14]. Fig. 3 shows this in an analytical and statistical study of WT fault [15]. A study is conducted in 2018 that analyzes the collected data related to the ReliaWind project, the results of which are shown in Fig. 4 [16]. This result is based on information from more than 4,000 turbines. In new variable speed turbines, most of the faults are related to the rotor and power subsystems. In Fig. 4, the vertical axis on the left of the graph represents the percentage of the total fault rate per (fault/turbine/year) while the horizontal axis on the right shows the cumulative fault rate for each section marked with an orange line [17].

The purpose of this article is to provide a platform to test and improvement of these fault diagnoses and fault-tolerant modules. The availability and reliability of WTs are under the influence of components failure including gearbox, generator, back-to-back converter, main bearing, blades, and tower [18]. In this paper, to identify a different symptom of WTs fault, a HIL test rig for simulating turbine faults is provided; this test rig is a DFIG with a prime mover motor. The topology of the WT system is the same as Fig. 5. Similar to this test rig different setups have been developed in various universities and research centers [13]-[15]. Different faults including Rotor Electrical Asymmetry (REA), Stator Inter-Turn Short Circuit (ITSC), and an open circuit switch fault are applied to display the performance of the HIL setup. In stator WT generators, the failure rate is 30%, the rotor has a failure rate of 40% and the bearing has a failure rate of 12%. In this article, the defects of the rotor winding are investigated. The fault of the rotor screw system is due to the manufacturing method, mechanical and thermal stresses, and current leakage [18[, [19]. In [20], the rotor winding fault detection is performed based on the analysis of current spectra. In [22], the rotor winding error is performed based on the analysis of current spectra. In [21], the rotor winding fault is investigated based on the frequency spectrum of the power and current signals, the power signal has a better detection power. The use of model-based methods based on rotor winding modeling is described in [22]. Using frequency analysis and frequency-based rotor fault detection is the most common method for REA fault diagnosis [23].

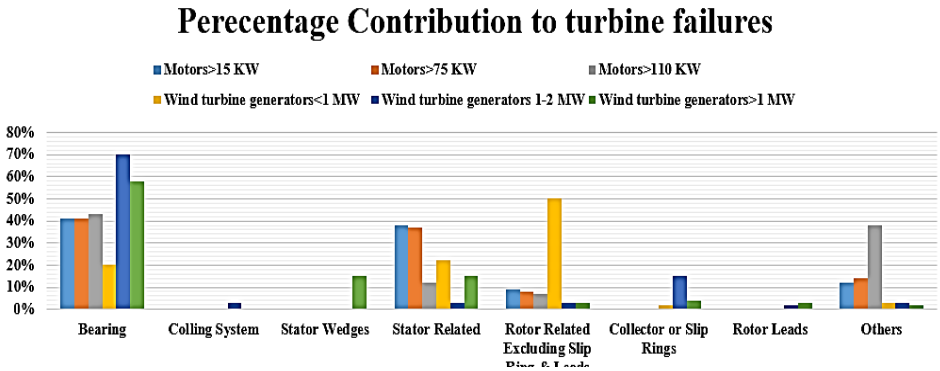

Fig. 3: Relationship between turbine power and separately component fault percentage [15].

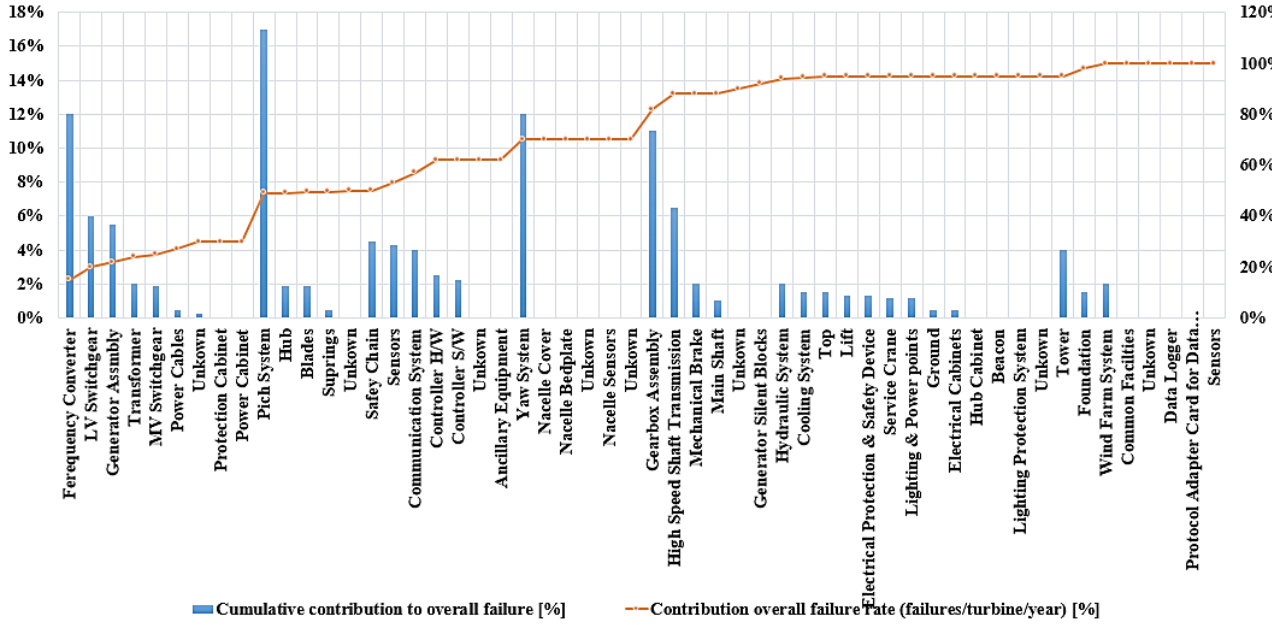

Fig. 4: Expansion of normalized outages related to WT subdivisions and different manufacturers in the analysis of the WT project carried out in 2017 [15].

These two signals are used in [24], [25] based on two generators for the error studied in the paper. But this REA fault causes certain changes in the frequency spectrum of current and power signals. These frequencies are a ratio of the main frequency of the source and depend on the fraction slip of the generator.

The most important frequency is $2sf_s$ [24], which is very efficient for REA fault detection. These frequencies are proportional to the different types of rotor and stator current signals and the control current signals are reflected in Fig. 6 [23], [26], [27]. The second case study fault is related to the stator. Generally, in induction machines including the DFIG, the ITSC fault, which damages the insulation of windings, is common [28]-[30]. Detecting this fault prevents the expansion of the fault. Faults that are related to the winding insulation have weak signatures in signals and their detection is more difficult than other faults [30]-[32]. Moreover, the variable speed of the WT and its unstable dynamics cause disturbances in current signals and make the FD very difficult. Few types of research related to ITSC fault in DFIG-based WTs have been conducted so far. However, many types of research have been conducted about this fault in induction motors [9]-[13]. Forty percent of the electrical faults in WTs are related to the generator, and 40% of these faults are due to faults in the stator [28]. Investigating the faults related to stators shows that the fault of windings is the most important fault in stators. Damage to the insulator occurs due to ITSC, and partial discharge takes place between stator turns. The latter leads to an inter-turn fault and emerges largely in the form of some kind of faults, such as coil-to-coil, phase-to-phase, open-circuit phase, and phase-to-ground, which may result in WT shutdown [32].

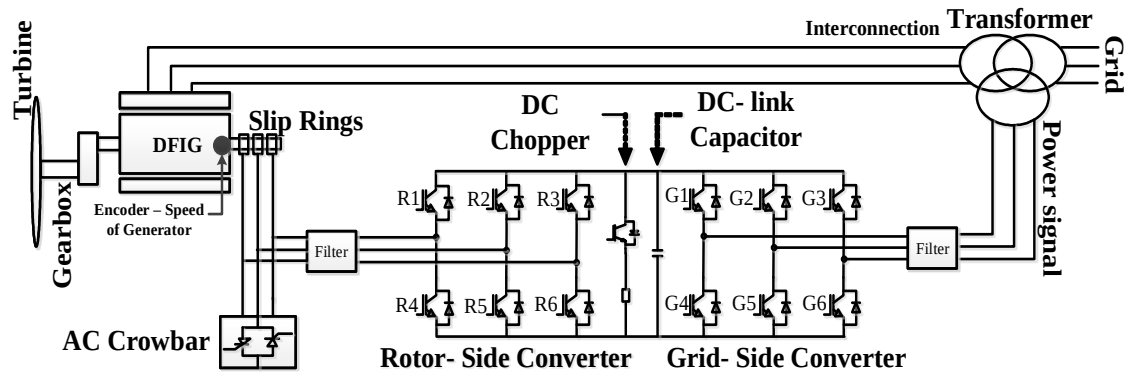

Fig. 5. WT DFIG topology

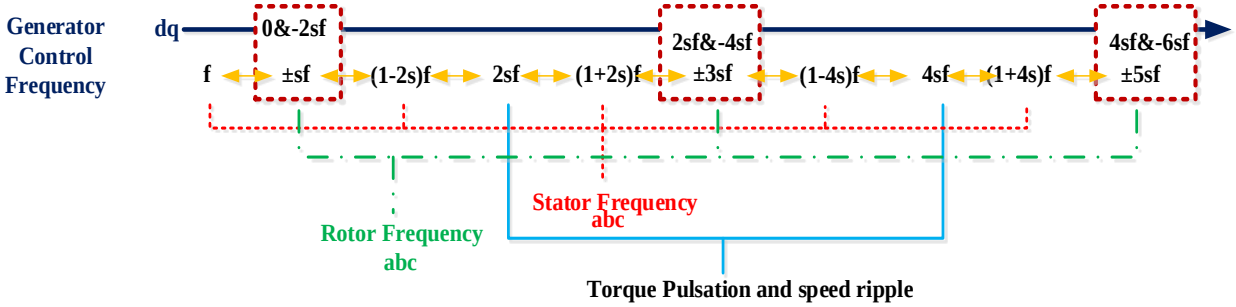

Fig. 6: The REA fault symptoms in frequency-domain.

This fault has little effect on the performance of the machine, and therefore, it can hardly be observed through the performance parameters of the WT; however, its development is very costly and destroys the generator. In Table 1, an appropriate description of various conditions of fault in the stator windings is presented [30]-[32].

Table 1: Various conditions of fault in the stator windings

State	Action
inter-turn short circuit	The generator will continue to operate, but for how long?
Shorts between coils of the same phase	The generator can continue to operate but for how long?
Phase to phase short	The generator fails and protection equipment disconnects the supply
Phase to earth short	The generator fails and protection equipment disconnects the supply
Open circuit in one phase	The generator may continue to operate, depending on the load conditions

Third case study fault related to the back-to-back converter. Power converter or back-to-back converter fault rates in DFIG and PMSG WT are high, in power converters nearly 35% of faults are due to IGBT switches, these faults are often due to mechanical stress, gate control circuit faults, thermal stress, wiring, and current problems [34]. There are two faults in the WT converter, an open circuit fault, and a short circuit fault. Unlike open circuit faults, which are often solved by software, the short circuit fault of the IGBT switch is often controlled by hardware, the short circuit fault is controlled by the WT protection system, and the WT is turned off, but The fault of the open circuit of IGBT WT converter does not cause the WT to down, but it is effective in the operating conditions of the WT, such as power quality, disturbance of balance and balance between phases [34]. Open circuit failure will cause offset current leakage in the phases, especially the phase related to the same switch. Except for offset and field, it produces jumps in torque and stator current frequency, which reduces the maximum average available for the drive, and of course, this affects power and other performance factors. Of course, the offset current also causes problems in the IGBT characteristics, and this may cause secondary defects and damage to the entire converter structure [34].

The reliability and availability concept is one of the most important issues in the WT industry, where unforeseen downtime can lead to significant economic losses. Fault diagnosis and fault-tolerant approaches are typical methods to reduce the cost of energy production and downtime of WTs. The doubly-fed induction generator converter Fault-Tolerant Control (FTC) plays a significant role in improving the reliability and availability of modern WTs. This article deals with the development of a 90 kW wind turbine simulator based on the DFIG

generator to be used in wind turbine fault diagnosis applications. In this context, intermittent Different faults and failures with different domains can be implemented and controlled in a single and combination format. To check the results and performance of the developed simulator, three categories of errors were checked. The first category of faults is related to defects in the rotor winding. Different faults including REA, Stator ITSC, and an open circuit switch fault are applied to display the performance of the HIL setup. The second case study fault is related to the stator. And finally, the Third case study fault is related to an open circuit fault in the back-to-back converter. The experiment shows that the CBM is improved by the proposed simulator and the fault is modeled before serious damage occurs. This setup is effective for the development of wind turbine fault analysis software. As the testing on real WTs is very expensive, to improve and develop the research fields of condition monitoring and WT control, this low-cost setup is effective.

The contributions of the article are categorized into four main parts.

- For fault diagnosis and Fault-tolerant control, hardware in the loop setup is proposed in this paper.
- The developed structure is quite similar to a real wind turbine; this makes it possible to examine fault and control issues.
- Simulate the actual behavior and dynamics of the WT based on the HIL test setup and perform experiments based on collecting real signals.
- The developed laboratory setup is prepared to emulate three faults; REA, IGBT open circuit fault, Stator ITSC.

The best parts of this paper are organized as follows: the second section is the system design for fault analysis. The third section has introduced the simulator. In section 4, fault representation is described. HIL performance analysis is presented in section 5 and finally, the last section is the conclusion.

HIL (Test Rig) Design for Fault Analysis

The WT hardware simulator platform is used in the developed loop to emulate faults and collect WT signals. In this context, intermittent faults and failures with different domains can be implemented and controlled in single and combination formats.

The fault prediction and detection and fault tolerant control algorithms can be implemented in this hardware. The general structure of the developed hardware simulator is shown in Fig. 7. As can be seen, this structure includes mechanical measurement sections, electrical measurement sections, and a control section.

The important components of the implemented structure are as follows:

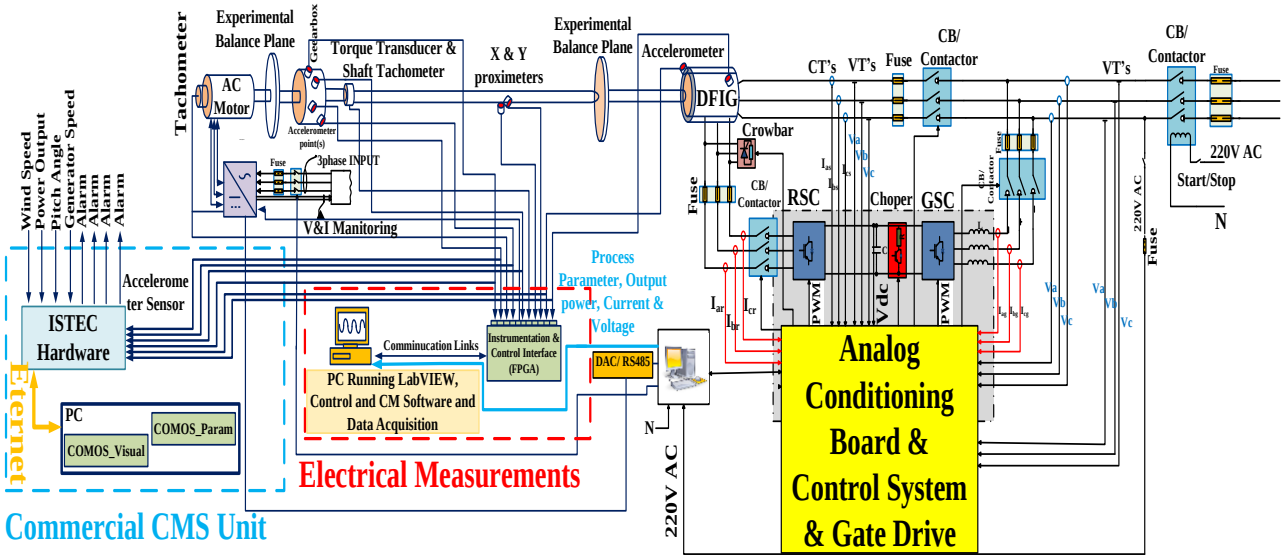

Fig. 7: Schematic diagram of the test rig.

ISTEC hardware for vibration monitoring (2) Accelerometer sensors to measure vibration intensity (3) A PC to install CMS software (Param and Visual) (4) Tachometer to measure generator speed (5) AC motor as the prim mover of the system (6) Shaft balancing plate to detect imbalance and failure in communication shafts between motor and gearbox (7) Torque measurement based on transducer (8) Variable speed driver with programmable ability to drive the motor (9) Drive input information monitoring system (10) Shaft balancing plate to detect imbalance and failure in communication shafts between generator and gearbox (11) Circuit breaker (crowbar) to protect against high leakage current (12) Current and voltage measurement sensors (13) Fuses and contactors in different directions (14) Power converter with stator side voltage source drive and rotor side voltage source drive (15) Analog and digital measuring boards (16) Central control board (17) Transformers (18)

DC link capacitor and related inductors. The MAPNA HIL system is included a generator from the VEM brand, this generator is operate with 90 kW power. The one gearbox is between the generator and primmover ABB motor (power: 110 kW). The system can be used to simulate converter and generator faults. An overview of these three interconnected devices is shown in Fig. 8. The system is capable of operating at constant and variable speeds. The primary drive motor is designed so that the DFIG generator operates with 4 pairs of poles in synchronous, sub-synchronous, and super-synchronous operating areas. For this purpose, the motor speed is 750 rpm with a grid frequency of 50 Hz 8 poles are selected. The gearbox conversion ratio activates the DFIG generator at a synchronous speed of about 1500 rpm in all three operating areas. The hardware simulator generator is 8 poles and can operate at 50 Hz and 400 volts. The HIL proposed in the paper is designed to simulate WT behaviors and simulates real similar signals and situations. Defects similar to WTs can be created in it or a defective condition can be removed from it, its prominent feature is the modeling of both faults in the electrical, mechanical and electro-mechanical parts.

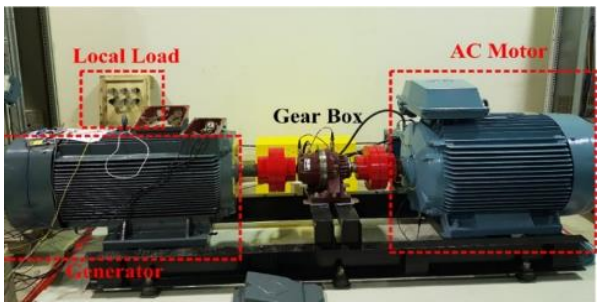

Fig. 8: DFIG WT test rig.

Table 2 shows the hardware simulator parameters.

Test Rig Mechanical and Electrical Components

A. Generator

In DEFA-based WTs, the generator power is often more than 2 MW; In this setup, a 90 kW DFIG is used to simulate a WT. This simulator requires upstream control and control at the converter and generator levels.

To simulate the fault, the winding rotor model must be considered, so a model based on the resistance bank for the rotor is used. In Fig. 9, this model is for the rotor. speed and sub-synchronous and super-synchronous. An external resistor is used to emulate the fault instead of the short circuit.

In the healthy state, the resistance of the three phases of the rotor is Balanced, this balance is disturbed by the addition of resistance. In balanced mode, the slip changes are small, and with the addition of this resistance, these changes are intensified. In this paper, the rotor phase resistance at NON- asymmetries IS 1.3 Ω. This amount is due to the WT SETUP being in synchronous.

Table 2: Parameters of test-rig components

Drivetrain	
Power	90 KW
Speed	1488RIV/MIN
Stator Voltage	400V
DC Link Voltage	700V
Current	199 A
Torque	578 Nm
Number of pole pairs	4
Magnetizing inductance	120.4 mH
CosΦ	0.88
Stator resistance	24.8mΩ
Stator inductance	44mH
Rotor resistance	16.6 mΩ
Rotor inductance	33mH
Gearbox	Gear with 1 stage by 1:3.32
Prime mover motor	8 pole / 110 kW/ 400 V/ 742 rpm
Converter	
Filter resistance	5mΩ
Filter inductance	800μH
Sampling frequency	100 kHz
Switching frequency	2.5 kHz
Converter control	FOC
DC-Link Capacitor	7 mF

B. Gearbox

The gearbox in the designed setup can be detached and a new gearbox replaced. This gearbox has a solar structure in the form of a parallel shaft. The output of the gearbox is a high speed and its input is low speed therefore the gearbox increases the distance. his gearbox is used to emulate various gear and bearing faults. The gearbox is coupled to the motor and generator in such a way as to prevent intrinsic vibration and achieve the main fault by measuring the signals. In [4], the presented method has been compared with other methods.

The HIL simulator receives wind speed maps and signal samples using a motor drive; the corresponding drive can receive a fixed map or a constant wind speed. This drive also can convert wind speed data to torque as a reference for variable speed motor performance and thus variable speed performance of WT hardware simulator.

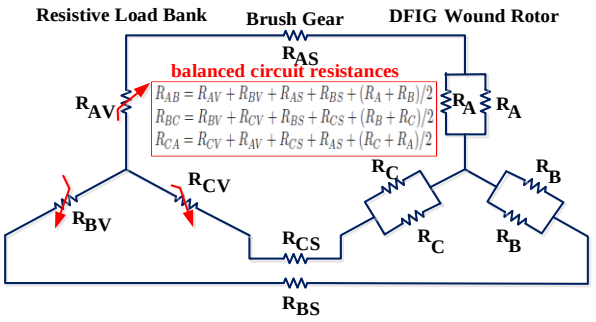

Fig. 9: Generator rotor circuit diagram.

C. Power Converter

In proportion to this input, the drive applies a certain frequency to each wind speed data to the motor. This drive capability allows the implementation of the plan to change the operating areas of the WT and transient conditions. The corresponding control cabinet is shown in Fig. 10 and the upper part of this cabinet contains the relevant drive. The lower part of this cabinet is ISTEC CMS. The back-to-back converter cabinet used in this structure is in Fig. 11. The system consists of two drive-based voltage sources in a back-to-back form, its power is 30 kW, a capacitor bank, and an output filter of 800µH-5mΩ, receptively. The DC link voltage of the converter is 700 volts. In the design of the converter power board, 6 SEMIKRON switches with two IGBTs connected are used. There is a crowbar circuit to prevent a short circuit. The ARM/FPGA-based control with a sampling frequency of 100 kHz for A/D channels has been implemented using conventional PWM (six-leg control), the switching signals are generated at 2.5 kHz frequencies and transmitted via fiber optics to the gate drive and applied to the IGBT, 12 gate drives are used for driving of 12 SEMIKRON switches. The vector control strategy is used for the converters, the control strategy is field vector control that which is based on space vector modulation for rotor and grid side converters.

D. Measurement Devices

To measure the signals required in this paper, a structure similar to Fig. 12 is used. A tachometer is used for measurement of the rotational speed of the generator and it is measured as input to the CMS. The control signals required on the control board are stored in the FPGA data archiving unit. Hioki power analyzer measures current/voltage information of three-phase, power information is measured through ISTEK CMS system. To achieve the research objectives, various measurements are designed in the hardware simulator.

Based on this structure, the rotational speed of the generator is used in the status monitoring and diagnosis process. This signal is measured using a tachometer. CMS measures the vibration signals from this hardware simulator as follows with 8 sensors.

Vibration sensors are accelerometers. The sensors are of the accelerometer type with a measurement accuracy specified by a magnet connector to a specific location on the hardware simulator and measure the vibration of the hardware simulator.

1. Two sensors are located at the end of the drive motor to indicate that the sensors are located in the main bearing of the WT before the gearbox low-speed shaft.
2. Four sensors are located at the gearbox similar to the location of the real gears.
3. Two accelerometer sensors are located on the generator at the beginning and end of the generator similar to the real situation in the WT.

Table 3 shows the general information of the hardware simulator measuring equipment.

E. CMS

MAPNA Kahak wind farm currently uses ISTEC CMS. This system is only for collecting information and calculating some frequency functions and time functions. It is the situation to do this offline, performance information including power, wind speed, generator speed, and step angle is received as the primary parameters from the control unit in the CMS system. Analysis should be performed taking into account the operating condition of the WT.

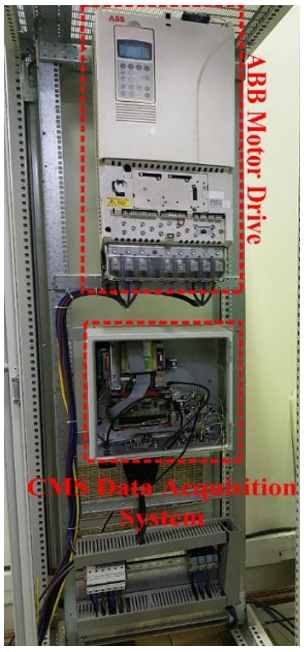

Fig. 10: Test rig instruments: prime mover motor drive and CMS.

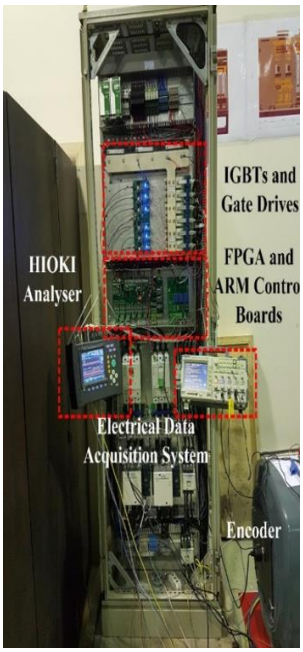

Fig. 11: Back-to-back converter.

Fig. 13 shows the condition monitoring hardware. The same system is also installed on the rig test. This system uses 8 accelerometer sensors, which are located according to Fig 14. 8 sensors are installed in the components of the gearbox (4), generator (2), and main bearing (2).

Table 3: The HIL test rig measuring devices

Hioki Power Quality Analyzer		WT CMS	
Input specifications			
Measurement line types	Single-phase 2-wire, Single-phase 3-wire, Three-phase 3- wire (3P3W2M, 3P3W3M), or Three-phase 4-wire, plus one extra input channel	Input channels	Time processing command variables up to a maximum of 4 channels (power, pitch angle, wind speed, generator speed)/ 8 acceleration sensors (Vibration channels)
Input channels	Voltage: 4 channels (U1 to U4) (channel U4 can be switched between AC and DC) Current: 4 channels (I1 to I4)		
Measurement specifications			
Current	calculated continuously every 10 or 12 cycles at 50 or 60 Hz respectively)	System architecture	
Measurement	2 MHz sampling	Measurement	32 kHz
Sensors	Clamp on Sensors: 1000 A AC, 1000 A continuous	Sensors	8 ICP acceleration sensors 10 mV/ms-2

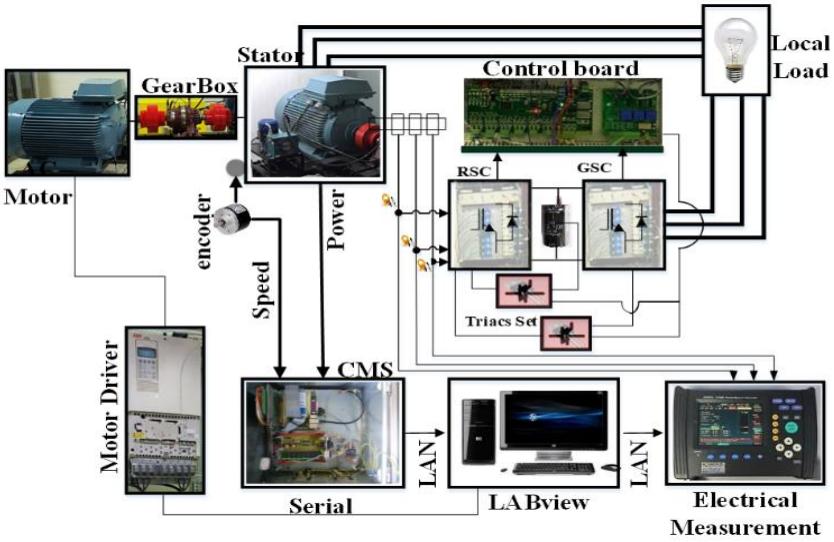

Fig. 12: The data collection system and HIL setup communication.

The system uses time-frequency and frequency domain analysis and statistical analysis performed inside the hardware to process the received signals. This product has proprietary software for hardware settings. This product has other software for statistical and graphical analysis. This system was launched about two years ago with the participation of the research author on the MAPNA Kahak site, and now the data collection of vibration signals from WTs on the Kahak site is underway. Also, this system is launched in the MAPNA WT laboratory and is installed on the WT test rig. The hardware of this system is a PC that operates upstream and has a DSP unit in which time and frequency domain functions are implemented. This system calculates the functions of maximum value, minimum value, crest, kurtosis, mean, and histogram from the time domain. Also, in the frequency domain, FFT is the main function and its output in the software can be seen at different time intervals.

Fig. 13: CMS hardware.

Fault Representation

A. Rotor Electrical Asymmetries (REA)

This fault is caused by an increase in the resistance that is series connected to the rotor winding [18]. Each of the winding and brush sections is modeled with a resistor, and the added resistor forms three series resistors for each phase.

Fig. 14: Location of vibration sensors of MAPNA WT condition monitoring system.

The corresponding schematic is shown in Fig. 9. It is also shown in the figure of total resistors [19]. Resistors R_{ea}, $R_{eb}$and R_{ec} are the same external resistors added, when the balance is disturbed in three-phase when one of the resistors is larger than the other two resistors. At balances, (1) is established, and (2) indicates an imbalance:

$$R_{ec} = R_{eb} = R_{ea} \quad (1)$$

$$R_{ea} = R_{eb} + \delta R = R_{ec} + \delta R \quad (2)$$

where δR is the amount of resistance added due to the asymmetry fault. An asymmetry is created in the same way in the desired simulator. The electrical asymmetry of the rotor can be defined as follows:

$$\delta R = \left|R_{1af}e^{i\theta_1} + R_{2bh}e^{i\theta_2} + R_{3ch}e^{i\theta_3}\right| \quad (3)$$

Where $i = \sqrt[2]{-1}$ ،$\theta_1 =?$,$\theta_2 = \frac{2\pi}{3}$ ،$\theta_3 = \frac{4\pi}{3}$.

in (3), h indicates a healthy state and f is a faulty condition. On the other hand, the degree of electrical asymmetry is determined by the following equation:

$$\Delta R(\%) = \frac{\delta R}{R_{1ah}} \times 100 = \frac{\delta R}{R_{2bh}} \times 100 = \frac{\delta R}{R_{3ch}} \times 100 \quad (4)$$

in (4) with resistance changing at various levels, different faults can be emulated. Based on (4), this fault percentage is determined [6]-[8]. In [5], [19] the presented method has been compared with other methods.

B. Inter-Turn Short Circuit (ITSC)

The ITSC fault causes damage to the stator winding insulation in the generator in the area between the coils. Condition monitoring and FD methods in induction devices are based on current analysis. In the stator current signal, (5) shows the fault frequency component in the corresponding spectrum.

$$f_{st} = f_1[{}^{n}/_{p}(1-s) \pm k] \quad (5)$$

where f_{st} is the frequency component, f_1 is the supply frequency, n = 1,2,3…, k = 1,3,5, and p is the pole pair and frictional slip is denoted by s. According to this equation, the frequency of the fault depends on the slip. In transient conditions, s is changing, therefore, it is difficult to detect a fault in the s variable. When there is an imbalance on the DFIG stator side, a negative harmonic component at the $-f_1$ of the stator produces a magnetic field. This magnetic field produces a harmonic component at the frequency (2-s) f_1. If in the frequency domain this fault is checked in the rotor current signal, the symptom of this fault component is the frequency $(2K \pm s)f_1$. The stator winding has a constant amplitude voltage. This voltage is connected directly to the grid. This voltage has a frequency equal to f_1. The DFIG rotor winding is connected to the generator via a back-to-back converter. After the stator ITSC fault occurs, a regular periodicity occurs in the positive and negative directions, with the corresponding frequencies at $f_1$and $-f_1$. Therefore, the grid voltage or stator voltage will create a new frequency component $2f_1$in the active and reactive power. This frequency has an amplitude of more than twice the power control loop and is well reflected in the signal. Because the ITSC fault occurs due to insulation damage between the loops of a coil, it is modeled as a short circuit in the coil, which affects the current stability. This modeling is based on Fig. 15.a. For this purpose, it is assumed that in modeling, the impedance of the shorted stator winding stator decreases. The amount of this reduction is related to the severity of the fault. Hence, in the simulator, a variable resistor, similar to Fig. 15.b, is placed parallel to one of the legs. The number of short-circuit loops is determined by the changes in this resistance.

C. Converter IGBT Open-circuit

To open the switch circuit, the gate cut of each switch is used [34]. For each side of the converter, there are six switches similar to Fig. 16. The manual switches shown in Fig. 16 are a solution for testing gate IGBT Open-circuit fault. To implement the hardware structural fault-tolerant scenario, a TRIAC circuit is used; this board receives commands from the main control board of the converter (similar to Fig. 12).

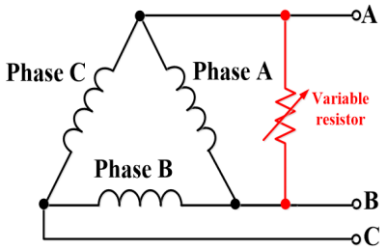

(a)

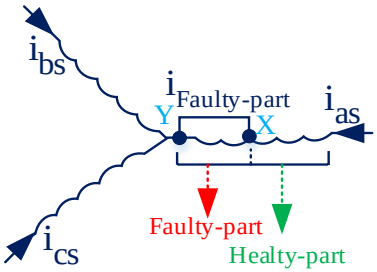

(b)

Fig. 15: Stator winding structure despite a fault in a winding phase.

Experimental Results and Discussion

A. Performance Analysis

To show the condition of the converter, Fig. 17 shows the thermal status of the switches and their switching condition. The general outputs of the HIL simulator, including the ratio of the generator speed diagram to the motor speed, and the generator speed diagram to the output power, are shown in Fig. 18 and Fig. 19, receptively. In Fig. 18, the gearbox conversion ratio will determine the generator speed. Generator speed is measured as one of the inputs of the CMS equipment channel.

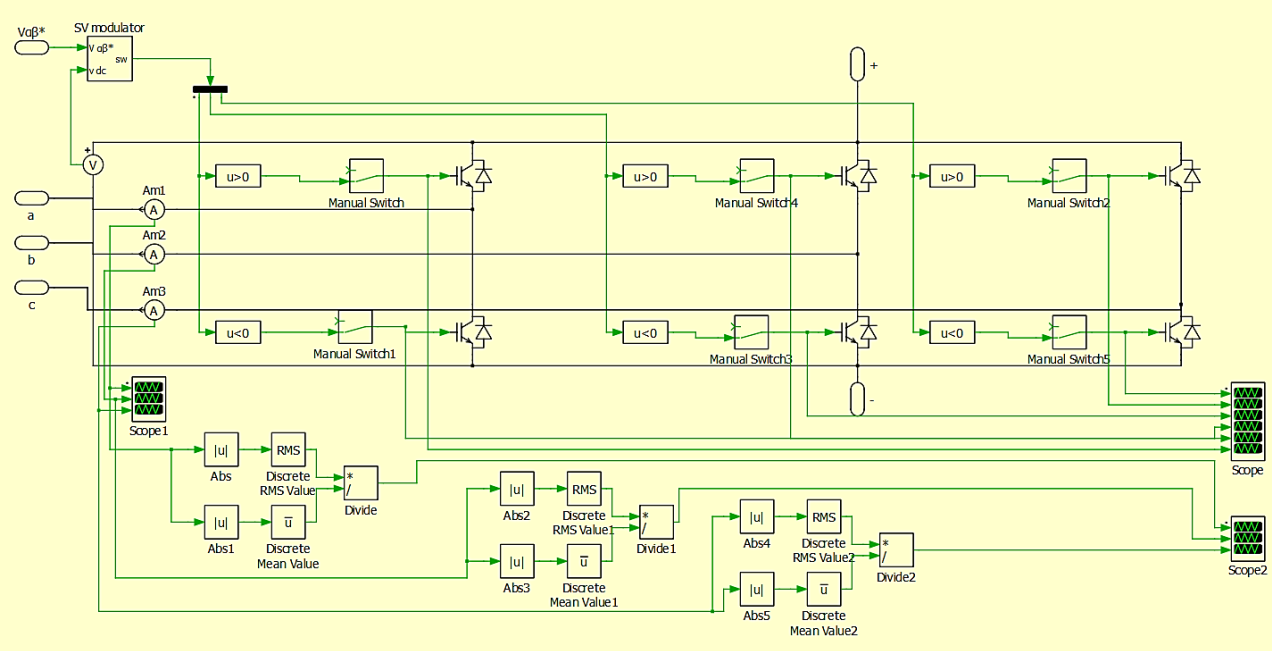

Fig. 16. schematic representation of converter IGBT open-circuit hardware implementation in WT test rig.

The motor speed is read from the drive and the generator speed is read from the CMS. Fig. 19 shows the WT HIL power generation performance. This diagram is based on the collected information about the power and speed of the generator, which is measured through the CMS.

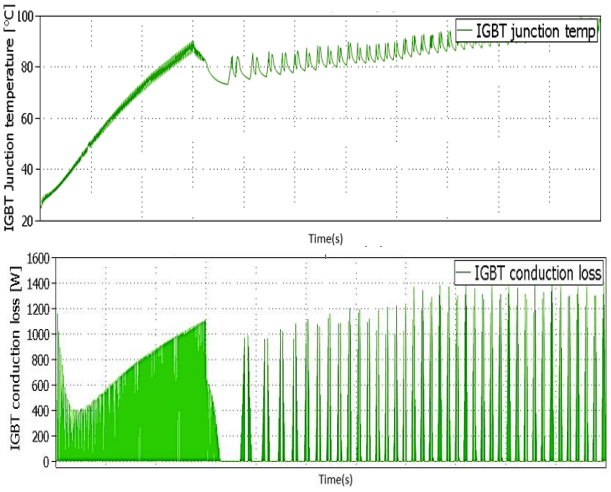

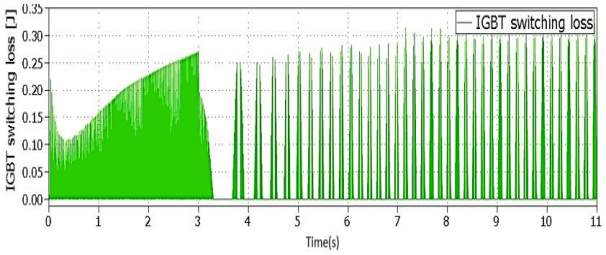

Fig. 17: IGBT status output in the back-to-back converter.

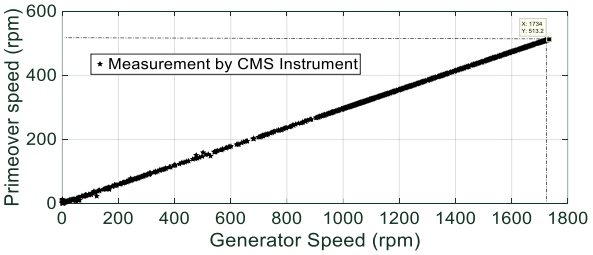

Fig. 18: Diagram of the motor prim mover speed of the motor than the generator speed.

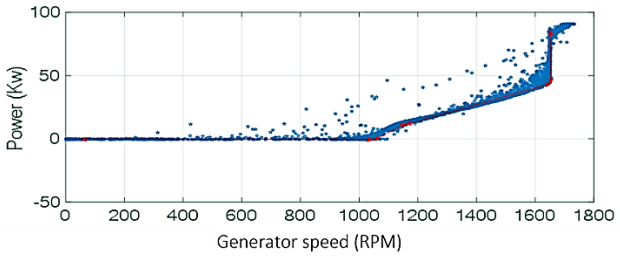

Fig. 19: WT HIL simulator power generation diagram based on generator speed.

B. Rotor Fault

Rotor asymmetries mean a fault in the rotor winding is simulated, which includes the effect of a fault in the winding, a brush imbalance, or an air gap imbalance on the rotor of a DFIG generator. Different levels of asymmetries are analyzed to measure the effect of the fault. These levels are shown in Table 4. The test is performed at different speeds from the WT HIL operating areas. The generator speed is from 1220 to 1600. This generator speed will be extracted through the wind speed pattern generated by the drive motor. To implement the experiments, some parameters must be set, for the power signal ω_c is equal to 2sf and for the stator current signal this value is equal to ((1-2s) f.

The time-domain signals are extracted in this experiment based on Fig. 20. A. From this figure, due to generator variable speed, It is clear that the fault symptom cannot be detected from the generator current (Fig. 20.a) or the power output (Fig. 20.d) of the generator. Generator rotation speed (Fig. 20.b), mechanical torque (Fig. 20.c), single-phase stator current (Fig. 20.a) and total power signal (Fig. 20.d) are measured from the simulator. The stator current frequency ((1-2s) f) at faulty condition (Fig. 20.e) and the fault frequency (2sf) (Fig. 20. f) for the power output are extracted. The variation of power and current signals is like the behavior of the generator rotation speed signal. Degradation of the generator fraction slip causes a change in the corresponding fault frequency.

Table 4: Rotor electrical asymmetries applied to DFIG generator

Time (s)	Condition	$\Delta\mathbf{R}$(%	Rotor resistance (m Ω)
0-50	Normal	0	16.6
50-150	Low asymmetries	9	18.09
150-200	Normal	0	16.6
200-300	Medium asymmetries	20	19.92
300-350	Normal	0	16.6
350-450	High asymmetries	46	24.23
450-500	Normal	0	16.6

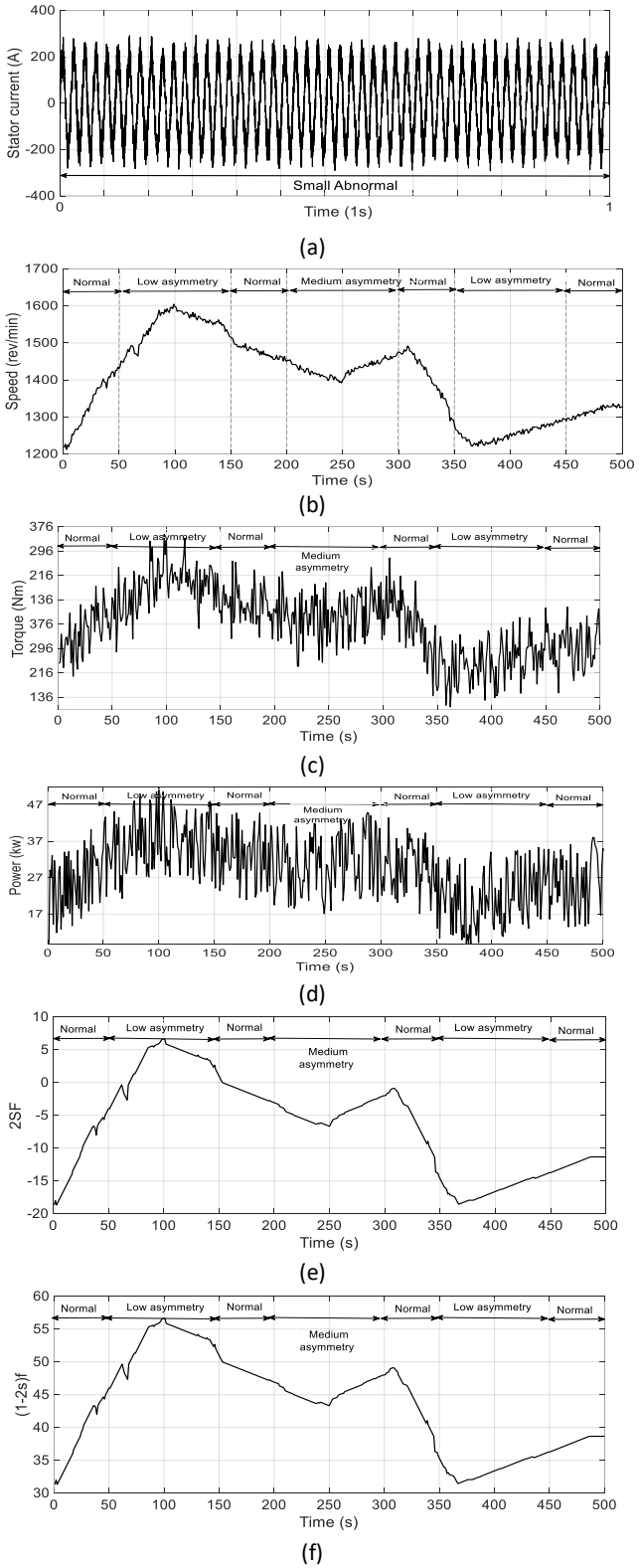

Fig. 20: The experimental result from WT HIL in the rotor fault condition.

C. Stator Fault

Table 5 shows the phase difference between the three stator phases for different fault values in the phase. For example, the failure rate in phase A increases the difference between phases A and B. While the phase

difference between the two healthy phases is very little (close to 120 degrees). Table 6 shows the complete harmonic distortion change. In this table, it is clear that the fault percentage increases with THD, but in the other two steps, the fault percentage changes are small and close to THD in a healthy state.

Table 5: Phase difference between the three phases of the stator in the presence of the fault

Fault Percentage	AB	BC	CA
Normal	120.012	1120.063	119.358
5	122.747	120.087	116.996
10	125.536	120.997	113.467
25	135.096	119.667	105.237
40	142.198	119.558	98.244

Table 6: THD changes in different fault percentages

Fault Percentage	C (%)	B (%)	A (%)
Normal	3.20	3.54	3.39
5	3.22	3.57	3.62
10	3.18	3.65	3.92
25	3.23	3.52	5.59
40	3.39	3.48	7.98

D. Converter Fault

By disconnecting the gate signal from the gate drive and removing the signal related to the gate, an open-circuit defect is created. Fig. 21 shows the experimental results of generator rotor currents. First, by disconnecting the driving signals of the IGBT gates S1 and S4 in 2.441 and 2.521 seconds, respectively, an open circuit fault occurs in one phase. With the IGBT open circuit fault, the current in the phases is damaged and distorted. This increases heat loss and vibration in the stator shaft. These behaviors and problems are exacerbated by the second open circuit fault. Fig. 22 shows the results obtained for the open circuit fault of the two IGBT switches S3 and S2 in 4.322 and 4.486 seconds on the grid side, respectively.

In [3], [19], [35], the presented method has been compared with other methods.

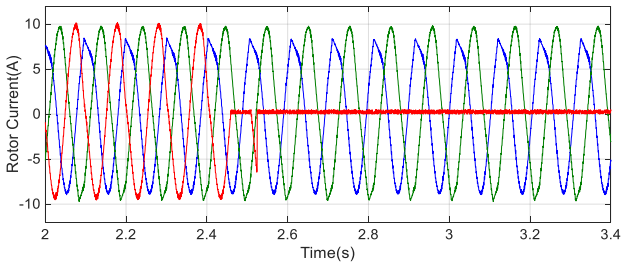

Fig. 21: Rotor current in presence converter fault.

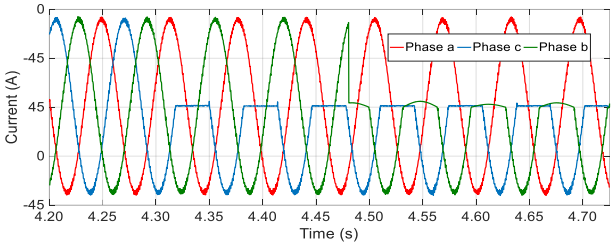

Fig. 22: Stator current in presence converter fault.

To provide more examples for verification and review of the presented results, you can refer to [36], [37].

More details of the implemented method, including relations, simulations, implementations, results, and their review are presented in [3]-[5], [19], [35]-[37].

Conclusion

In this paper, a hardware simulator for WTs is presented. This hardware in the loop is designed and launched in the research and development laboratory of MAPNA Group. The need to develop a simulator to investigate faults in WTs and their monitoring methods are first considered, an analysis of the types and percentages of faults in WTs is presented, the test rig structure is described and its subsystems are investigated. Fault generation and scenario-building solutions in the test bench are analyzed for the rotor, stator, and converter faults, and finally, an analysis of the performance of the test rig in the presence of a fault and healthy condition is presented. This structure can be used to develop new fault diagnosis software, fault prediction, and fault-tolerant control methods. Testing on real WTs is very expensive, but using this low-cost setup is effective to develop and improve the field of condition monitoring and WT control.

Abbreviations

CBM : Condition Based Maintenance
DFIG : Double Feed Induction Generator
FD : Fault Detection
FTC : Fault-Tolerant Control
HIL : Hardware In the Loop
ITSC : Inter-Turn Short Circuit
REA : Rotor Electrical Asymmetry
WTs : Wind Turbines

Acknowledgment

This article was prepared with the support of MAPNA Electric & Control, Engineering & Manufacturing Co. (MECO). Our MAPNA Group colleagues at various companies have assisted in this research. Thanks to them, of course, does not mean that they agree with all the results of the article and the authors are responsible for the results of the article.

Author Contributions

M. Kamarzarrin, M.H. Refan, P. Amiri, A. Dameshghi had role in Conception and Design. M. Kamarzarrin, A.

Dameshghi did Data Acquisition, Analysis and interpretation of data, Manuscript Drafting, and Statistical Analysis. M.H. Refan, P. Amiri, and A. Dameshghi had a role in Administrative, Technical, or Material Support. Obtaining Funding was with M.H. Refan.

Conflict of Interest

The authors declare no potential conflict of interest regarding the publication of this work. In addition, ethical issues including plagiarism, informed consent, misconduct, data fabrication and, or falsification, double publication and, or submission, and redundancy have been completely witnessed by the authors.

References

[1] M. Kamarzarrin, M. H. Refan, "Intelligent sliding mode adaptive controller design for wind turbine pitch control system using PSO-SVM in presence of disturbance," J. Control Autom. Electr. Syst., 31(4): 912-925, 2020.

[2] M. H. Refan, A. Dameshghi, "A new strategy for short-term power-curve prediction of wind turbine based on PSO-LS-WSVM," Iran. J. Electr. Electron. Eng., 4: 392-403, 2018.

[3] m. kamarzarrin, m. h. refan, p. amiri, a. dameshghi, "Fault diagnosis of wind turbine double-fed induction generator based on multi-level fusion and measurement of back-to-back converter current signal," Iran. J. Electr. Electron. Eng., 18(2): 2074-2074, 2022.

[4] A. Dameshghi, M. H. Refan, "Wind turbine gearbox condition monitoring and fault diagnosis based on multi-sensor information fusion of SCADA and DSER-PSO-WRVM method," Int. J. Model. Simul., 39: 48-72, 2019.

[5] A. Dameshghi, M. H. Refan, "Combination of condition monitoring and prognosis systems based on the current measurement and PSO-LS-SVM method for wind turbine DFIGs with rotor electrical asymmetry," Energy Syst., 2: 1-30, 2021.

[6] J. M. P. Pérez, F. P. G. Márquez, A. Tobias, M. Papaelias, "Wind turbine reliability analysis," Renewable Sustainable Energy Rev., 23: 463-472, 2013.

[7] T. A. Kawady, A. A. Afify, A. M. Osheiba, A. I. Taalab, "Modeling and experimental investigation of stator winding faults in induction motors," Electr. Power Compon. Syst., 37: 599-611, 2009.

[8] D. Zappalá, N. Sarma, S. Djurović, C. J. Crabtree, A. Mohammad, P. J. Tavner, "Electrical & mechanical diagnostic indicators of wind turbine induction generator rotor faults," Renewable energy, 131: 14-24, 2019.

[9] M. Wilkinson, B. Darnell, T. Van Delft, K. Harman, "Comparison of methods for wind turbine condition monitoring with SCADA data," IET Renewable Power Gener., 8: 390-397, 2014.

[10] F. Haces-Fernandez, H. Li, D. Ramirez, "Improving wind farm power output through deactivating selected wind turbines," Energy Convers. Manage., 187: 407-422, 2019.

[11] K. B. Abdusamad, Condition Monitoring System of Wind Turbine Generators. PHD thesis, University of Durham, 2014.

[12] K. Alewine, W. Chen, "A review of electrical winding failures in wind turbine generators," IEEE Electr. Insul. Mag., 28:8-13, 2012.

[13] J. M. P. Pérez, F. P. G. Márquez, A. Tobias, M. Papaelias, "Wind turbine reliability analysis," Renewable Sustainable Energy Rev., 23: 463-472, 2013.

[14] L. Alhmoud, B. Wang, "A review of the state-of-the-art in wind-energy reliability analysis," Renewable Sustainable Energy Rev., 81: 1643-1651, 2018.

[15] C. J. Crabtree, Condition Monitoring Techniques for Wind Turbines. PhD Thesis, Durham University, 2011.

[16] W. Hu, "Reliability-based design optimization of wind turbine systems," Advanced Wind Turbine Technology, Springer, Cham, 1-45, 2018.

[17] M. Yadav, P. Prakash, R. C. Jha, "Reliability analysis and energy benefit analysis of distribution system incorporating wind turbine generator," in Proc. the International Conference on Nano-electronics, Circuits & Communication Systems: 265-273, 2017.

[18] M. Kamarzarrin, M. H. Refan, P. Amiri, A. Dameshghi, "A new intelligent fault diagnosis and prognosis method for wind turbine doubly-fed induction generator," Wind Eng., 10: 210-221, 2021.

[19] A. Dameshghi, M. H. Refan, P. Amiri, "Wind turbine doubly fed induction generator rotor electrical asymmetry detection based on an adaptive least mean squares filtering of wavelet transform," Wind Eng., 8: 1-21, 2019.

[20] M. Kamarzarrin, M. H. Refan, P. Amiri, A. Dameshghi, "A new fault-tolerant control of wind turbine pitch system based on ANN model and robust and optimal development of MRAC method," Tabriz Electr. Eng. J., 51: 83-95, 2021.

[21] W. T. Thomson, M. Fenger, "Current signature analysis to detect induction motor faults," IEEE Ind. Appl. Mag., 7: 26-34, 2001.

[22] C. J. Crabtree, S. Djurović, P. J. Tavner, A. C. Smith, "Fault frequency tracking during transient operation of wind turbine generators," in Proc. XIX International Conference on Electrical Machines, ICEM 2010, Rome, Italy, 2010.

[23] S. Djurovic, C. J. Crabtree, P. J. Tavner, A. C. Smith, "Condition monitoring of wind turbine induction generators with rotor electrical asymmetry," IET Renew. Power Gen., 6: 207-216, 2012.

[24] X. Gong, Online Nonintrusive Condition Monitoring and Fault Detection for Wind Turbines. PHD Thesis, University of Nebraska, 2012.

[25] M. Yousefi kia, M. Khedri, H. R. Najafi, M. A. Shamsi Nejad, "Hybrid modeling of doubly fed induction generators with inter-turn stator fault and its detection method using wavelet analysis," IET Gener. Transm. Distrib., 7: 982-990, 2013.

[26] R. Roshanfekr, A. Jalilian, "Analysis of rotor and stator winding inter-turn faults in WRIM using simulated MEC model and experimental results," Electr. Power Syst. Res., 119: 418–424, 2015.

[27] R. Roshanfekr, A. Jalilian, "Wavelet-based index to discriminate between minor inter-turn short-circuit and resistive asymmetrical faults in stator windings of doubly fed induction generators: a simulation study," IET Gener. Transm. Distrib., 10: 1–8, 2016.

[28] P. V. Rodríguez, A. Arkkio, "Detection of the stator winding fault in induction motor using fuzzy logic," Appl. Soft Comput., 8: 1112–1120, 2008.

[29] R. Sharifi, M. Ebrahimi, "Detection of the stator winding faults in induction motors using three-phase current monitoring," ISA Trans., 50: 14–20, 2011.

[30] A. Bechkaouia, A. Ameurb, S. Bourasc, A. Hadjadjd, "Open-circuit and inter-turn short-circuit detection in PMSG for wind turbine applications using fuzzy logic," Energy Procedia, 74: 1323–1336, 2015.

[31] M. S. Ballal, Z. J. Khan, H. M. Suryawanshi, R. L. Sonolikar, "Adaptive neural fuzzy inference system for the detection of inter-turn insulation and bearing wear faults in induction motor," IEEE Trans. Ind. Electron., 54: 250-258, 2007.

[32] A. Djerdira, S. S. Moosavia, Y. Ait-Amiratb, D. A. Khaburica, "ANN based fault diagnosis of permanent magnet synchronous motor under stator winding shorted turn," Electr. Power Syst. Res., 125: 67–82, 2015.

[33] R. M. Tallam, S. B. Lee, G. C. Stone, "A survey of methods for detection of stator-related faults in induction machines," IEEE Trans. Ind. Appl., 43: 920-933, 2007.

[34] A. Dameshghi, M. H. Refan, "The fault diagnosis of open-circuit of back-to-back converters in dfig wind turbines of variable speed using combination signal-based and model-based methods," J. Energy Manage., 9: 18-33, 2019.

[35] M. Kamarzarrin, M. H. Refan, P. Amiri, "Open-circuit faults diagnosis and Fault-Tolerant Control scheme based on Sliding-Mode Observer for DFIG back-to-back converters: Wind turbine applications," Control Eng. Prac., 126: 105235, 2023.

[36] A. Dameshghi, "Wind turbine generator and converter maintenance based on smart monitoring based on data fusion strategy", Ph.D. thesis, Shahid Rajaee Teacher Training University, 2019.

[37] M. Kamarzarrin, "Enhanced Fault Tolerant of Dual Open-circuit Faults with Back-to-Back converter of DFIG Wind Turbine", Ph.D. thesis, Shahid Rajaee Teacher Training University, 2022.

Biographies

Mehrnoosh Kamarzarrin was born in 1991 and is receiving currently her B.S. degree (with the highest honors) in Electronic Engineering from Shahid Rajaee Teacher Training University (SRTTU), Tehran, Iran, in 2013. She received her M.Sc. in Control Engineering from Shahid Beheshti University, Tehran, Iran in 2015. Now she is a Ph.D. in Electronic Engineering at Shahid Rajaee Teacher Training University. Her research interests include GPS, wind turbine, fault detection & tolerant control, Adaptive control, wireless communications, and networking with a focus on cognitive radios, Analog electronics, and Boolean Function. Now she is the wind turbine process expert in MAPNA Electric & Control, Engineering & Manufacturing Co. (MECO).

- Email: kamarzarrin.mehrnoosh@sru.ac.ir
- ORCID: 0000-0003-2292-3861
- Web of Science Researcher ID: NA
- Scopus Author ID: 55975874300
- Homepage: https://ir.linkedin.com/in/mehrnoosh-kamarzarrin-aa353b58

Mohammad Hossein Refan received his B.Sc. in Electronics Engineering from the Iran University of Science and Technology, Tehran, Iran in 1972. After 12 years of working and experience in the industry, he started studying again in 1989 and received his M.Sc. and Ph.D. in the same field and at the same University in 1992 and 1999 respectively. He is currently a Professor of Electrical and Computer Engineering Faculty, Shahid Rajaee Teacher Training University, Tehran, Iran. He is the author of about 50 scientific publications in journals and international conferences. His research interests include GPS, DCS, and Automation systems, wind turbines, fault detection & tolerant control, and Adaptive control.

Email: Refan@sru.ac.ir
- ORCID: 0000-0001-5266-0586
- Web of Science Researcher ID: NA
- Scopus Author ID: NA
- Homepage: https://www.sru.ac.ir/en/faculty/school-of-electrical-engineering/mohammad-hossein-refan/

Parviz Amiri was born in 1970. He received his B.Sc. degree from the University of Mazandaran in 1994, his M.Sc. from Khajeh Nasir Toosi University (KNTU Tehran, Iran) in 1997, and his Ph.D. from Tarbiat Modares University (TMU, Tehran, Iran) in 2010, all degrees in Electrical Engineering (Electronics). His main research interest includes electronic circuit design in industries. His primary research interest is in RF and power electronic circuits, with a focus on highly efficient and high linear power circuit design. He is currently an Associate Professor of Electrical and Computer Engineering Faculty, Shahid Rajaee Teacher Training University, Tehran, Iran.

- Email: pamiri@sru.ac.ir
- ORCID: 0000-0001-5764-0912
- Web of Science Researcher ID: NA
- Scopus Author ID: NA
- Homepage: https://www.sru.ac.ir/en/faculty/school-of-electrical-engineering/parviz-amiri/

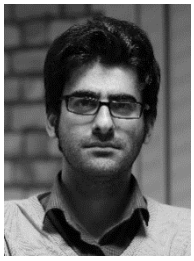

Adel Dameshghi was born in1986 and received his B.S., M.S. Ph.D. degrees in Electronic Engineering from the Department of Electrical Engineering, of Electrical and Computer Engineering, Shahid Rajaee Teacher Training University (SRTTU), Tehran, Iran, in 2011, 2013 and 2020 respectively. His research interests include Boolean Function, GPS, wind turbine, fault detection & tolerant control, Adaptive control, Electric, and Hybrid vehicles and now he is the manager of the EV & infrastructure Development Center of MAPNA Electric & Control, Engineering & Manufacturing Co. (MECO).

- Email: a.dameshghi@sru.ac.ir
- ORCID: 0000-0001-8764-4287
- Web of Science Researcher ID: NA
- Scopus Author ID: NA
- Homepage: https://ir.linkedin.com/in/adel-dameshghi-20617941

How to cite this paper:
M. Kamarzarrin, M. H. Refan, P. Amiri, A. Dameshghi, "Development of wind turbine fault analysis setup based on dfig hardware in the loop simulator," J. Electr. Comput. Eng. Innovations, 11(2): 277-290, 2023.

DOI: 10.22061/jecei.2022.8849.556

URL: https://jecei.sru.ac.ir/article_1809.html